Flexing the Default Barrier*

Gregor Dorfleitner† Paul Schneider‡ Tanja Veža§

December 18, 2008

Abstract

The paper introduces a Black&Cox-type structural model for credit default swaps. The existing literature on structural CDS pricing is extended by allowing a general functional form for the default barrier specified without reference to asset volatilities, dividend yields and interest rates. We develop a fast and robust algorithm to compute survival probabilities numerically. An empirical application suggests that the market-implied barrier is stable over time, with a possibly hump-shaped term structure. The implied barrier can be used for computing survival probabilities consistent with objective expectations of asset evolution, for pricing under counterparty risk, and for determining optimal corporate bond covenants.

JEL Classification: C13, G12, G13, G15

MS Classification: 62P05, 68W25, 91-08

Keywords: credit default swap, structural model, default boundary, the Green function, calibration

*Our thanks go to Hannelore De Silva and Klaus Pötzelberger for mathematical assistance.

†Gregor Dorfleitner, Department of Finance, University of Regensburg, Universitätsstraße 31, 93053 Regensburg, Germany, gregor.dorfleitner@wiwi.uni-regensburg.de

‡Paul Schneider, Finance Group, Warwick Business School, University of Warwick, Coventry CV4 7AL, UK, paul.schneider@wbs.ac.uk

§Tanja Veža, Institute for Banking and Finance, Vienna University of Economics and Business Administration, Heiligenstädter Straße 46-48, 1190 Vienna, Austria, tanja.veza@wu-wien.ac.at

1 Introduction

Until very recently, both academic and practitioners' studies in credit risk have predominantly employed intensity models for calibration and pricing purposes due to their good statistical properties when fitted to single-name corporate bond and/or credit default swap (CDS) data. A disadvantage of this approach, though, is that it does not relate the default trigger to an economic quantity, but rather to a latent jump process with an abstract jump intensity governing default probabilities. In contrast to the reduced-form approach, in the contingent-claim framework default primarily depends on the value of the obligor's assets during the lifetime of debt. This property enables taking further real-world features into account, such as taxes, bankruptcy costs, or safety covenants, as well as investigating optimal capital structure, expressing recovery values endogenously, studying the effects of lagging or incomplete accounting information, strategic debt service etc.

The basic Merton (1974) setup assumes a rudimentary firm capital structure consisting only of equity and one zero-coupon debt issue. At debt maturity the firm defaults if the value of its assets is not sufficient to pay back the debt. Our paper focuses on the default-barrier (also first-passage-time) setup pioneered by Black and Cox (1976). Their approach extends the simplistic Merton setup by allowing default anytime before maturity through the introduction of a lower boundary on assets triggering early default in case the firm slides into a bad state. Thereby the model takes into account safety covenants in an obligor's indenture provisions which provide its creditors with the right to force it to bankruptcy if it is doing poorly according to the boundary as benchmark. Further developments of this basic idea have gone in several directions, such as including interest rate risk through stochastic interest rates (Kim et al., 1993; Longstaff and Schwartz, 1995) and generalizing the form of the default barrier to account for the debt level (Briys and de Varenne, 1997; Hsu et al., 2002).

During the last few years several studies have emerged applying structural models in CDS pricing. These papers employ a specific functional form of the default boundary which still allows a closed-form expression for survival probabilities (Hui et al., 2003; Brigo and Tarenghi, 2005a,b; Brigo and Morini, 2006). Their default boundary implies exponential growth and explicitly and solely depends on asset volatility (apart from the exogenously given riskless short rate and dividend yield). CDS premia are thus fitted by the asset volatility function, resulting in implied asset volatility patterns inconsistent with typically observed equity volatilities. Refining the technique introduced in Dorfleitner et al. (2008), our paper proposes a flexible setup featuring an *arbitrary* default boundary function – its concrete functional form is specified without reference to asset volatilities, riskless interest rates or dividend yields, and admits upward and downward sloping as well as humped shapes.

Asset volatility does not enter our default boundary function directly, but it is still necessary for calibration because it appears in the firm value dynamics. Several recent papers have pointed out

the influence of historical and option-implied volatilities on CDS premia, e.g. Aunon-Nerin et al. (2002), Benkert (2004) and Berndt et al. (2008). In light of these findings we infer asset volatility from equity option prices, which has the advantage that asset volatility need not be fitted to CDS spreads any longer. In addition, since firm leverage links equity volatility to asset volatility, our method admits calibration of CDS premia consistent with both the option-implied volatility term structure and the current proportion of debt. The possibility to price consistently and calibrate sequentially across markets is a feature which presents a pronounced advantage of our methodology over existing related models.

Our approach uses the Green function to solve the Black-Scholes pricing PDE with time-dependent coefficients and boundary conditions, and originates from the numerical valuation of barrier options (cf. Rapisarda, 2003; Lo et al., 2003). Calibration is performed by a fast and precise numerical procedure tailored to the specific problem. An application of our method to two exemplary obligors yields the following stylized findings: Fluctuations in the implied barrier function on consecutive days are small, indicating the stability of our method. Level and slope of the CDS-implied default barrier are related to market perceptions of changes in the future financial situation of an obligor. A slight downward hump indicates that the rigid boundary form employed in previous papers, implying exponential growth, is not satisfactory and could possibly turn out misleading. In the short term, firm leverage emerges as a stronger influence on the default barrier than equity volatility.

The implied default barrier has several applications of both practical and academic interest. A typical one is the valuation of an equity-based cash flow from a defaultable counterparty (such as an equity default swap), in which case default correlation between underlying and counterparty must be taken into account (so-called vulnerable claims or claims with counterparty risk, cf. Brigo and Tarenghi, 2005a,b; Brigo and Masetti, 2005). Further, analysts' estimates of earnings per share together with information about the capital structure of a firm can be used in connection with our model to determine survival probabilities under the historical measure consistent with observed CDS premia and equity volatilities. This feature presents a major advantage of our model over a reduced-form one, where estimating objective survival probabilities is much more involved.[1] Furthermore, our barrier-implied survival probabilities under the historical measure can be used as a direct measure of default risk, whereby important determinants, such as the riskless yield curve, equity volatility, and capital structure are already controlled for (cp. Ericsson et al., 2007). Moreover, the analytic framework together with the numerical solution algorithm developed in this paper is capable of handling optimal-control problems. Our technique could therefore be employed for determining optimal debt covenants or endogenous refinancing times as modeled in Hilberink and Rogers

[1] An estimate of objective survival probabilities consistent with CDS premia using a reduced-form model demands knowledge of the drift in the default intensity under the physical measure. This drift can only be inferred from long time series of CDS premia, which do not exist in this relatively young market.

(2002), Dangl and Zechner (2004) or Detemple and Tian (2007).

The paper proceeds as follows: The next section describes how survival probabilities are expressed within our generalized first-passage-time model, as well as how CDS contracts are evaluated. Details about the numerical procedure are laid out in Section 3, together with estimates for approximation errors. The presented methodology is subsequently applied to two exemplary obligors, and findings are summarized in Section 4. Section 5 concludes.

2 Setup and Pricing

The main intention of the Black and Cox (1976) model is to extend the rudimentary Merton (1974) setup by allowing default to happen not only at the debt maturity, but also at any interim point in time. Thereby the model accounts for safety covenants in an obligor's indenture provisions which provide creditors with the right to force it to bankruptcy if it is doing poorly according to a set benchmark. In general mathematical terms, this feature is modeled by letting default occur if and when the process for the firm's asset value passes a prespecified boundary for the first time.

2.1 Default Model

We assume a continuous-time, Black-Scholes-type frictionless market. Uncertainty is modeled by a probability space $(\Omega, \mathcal{F}, \mathbb{Q})$, where $\mathbb{Q}$ denotes the risk-neutral (pricing) measure associated with the riskless money market account. Let the value y_t of the firm's assets be described by the following SDE under $\mathbb{Q}$:

$$\frac{dy_t}{y_t} = (r(t) - q(t))\,dt + \sigma(t)\,dB_t\,, \tag{1}$$

where B denotes a standard Brownian motion under $\mathbb{Q}$, $r(t) > 0$ the continuously compounded riskless short rate, $q(t) \geq 0$ the instantaneous (dividend) payout ratio, and $\sigma(t) > 0$ the instantaneous asset volatility. All coefficients are assumed to be deterministic functions[2] of time to increase the model flexibility in calibrating CDS market data. In particular, we assume a time-dependent, though deterministic short rate $r(t)$ – differently from Black and Cox (1976), who disregard term structure information by taking a constant riskless short rate. Thus, the time-t price of a risk-free zero-coupon bond maturing at time T may be expressed as

$$P(T|t) = \exp\left\{-\int_t^T r(s)ds\right\}. \tag{2}$$

In Black and Cox (1976) the standard for poor performance of the obligor is set by a time-dependent deterministic safety barrier of the form $K\exp\{-\gamma(T-t)\}$, $0 \leq t < T$, for some constants

[2] Additional technical requirements are integrability of functions r and q as well as square integrability of σ.

$\gamma, K > 0$. Default occurs when the firm's asset value falls below this level for the first time. Our model is a generalization of their setup in that we do not assume a fixed functional form for the default boundary, but allow it to be an arbitrary deterministic function $b(t) \geq 0$ depending on time. Our default time thus equals (as usual, $\inf \emptyset = \infty$):

$$\tau := \inf \{t \geq 0 : y_t \leq b(t)\} . \tag{3}$$

In applications we naturally impose $y_0 > b(0)$ and normalize the initial asset value y_0 to 1 for want of data, so future asset and barrier levels are expressed relative to the initial value of assets. Survival probabilities are thus determined by the distribution of the first passage time τ of the asset value y_t to the barrier $b(t)$. In what follows we develop a Green function approach to expressing survival probabilities within the first-hitting-time framework.

Let $\widetilde{P}(T|y,t)$ denote the time-t price of a defaultable zero-coupon bond with maturity T and zero recovery, given an asset value of y at time t. Intuitively, $\widetilde{P}(T|y,t)$ is the time-t value of a promised payment of 1 currency unit at time T paid in case of no default until then, i.e. in case the process for the firm's value never touches the boundary from above until maturity. There exists hence an analogy between a defaultable zero-coupon bond in the first-hitting-time setup, and a down-and-out digital barrier option. Such contracts pay 1 currency unit at maturity if the underlying price does not fall below a prespecified barrier meanwhile.

Consequently, within our generalized first-hitting-time setup we can make use of existing methods for pricing barrier options with the underlying following dynamics (1); we employ the methodology developed by Dorfleitner et al. (2008), who work with the following functional form for the barrier:

$$b^{\diamond}(s) = \exp\left\{ \frac{\tilde{\alpha}(t,T)\,\tilde{\beta}(t,s) - \tilde{\alpha}(t,s)\tilde{\beta}(t,T)}{\tilde{\alpha}(t,T)} \right\} \left(\frac{d}{c}\right)^{\frac{\tilde{\alpha}(t,s)}{\tilde{\alpha}(t,T)}} c \qquad \text{for} \quad t \leq s \leq T\,, \tag{4}$$

where $\alpha(s) := \sigma^2(s)/2 > 0$, $\beta(s) := r(s) - q(s)$, and

$$\tilde{\alpha}(t,T) := \int_t^T \alpha(s)\,ds\,, \qquad \tilde{\beta}(t,T) := \int_t^T \beta(s)\,ds \qquad \text{and} \qquad \tilde{r}(t,T) := \int_t^T r(s)\,ds \tag{5}$$

to lighten notation; $c, d \geq 0$ are arbitrary parameters representing the start and end points of the barrier, i.e. $b^{\diamond}(t) = c$ and $b^{\diamond}(T) = d$. The barrier $b^{\diamond}$ is termed the *natural barrier* since it represents the most general functional form still allowing a closed-form solution to the option pricing problem (up to numerical integration).

Dorfleitner et al. (2008) provide a closed-form solution for the time-t value function $v(y,t)$ of a down-and-out barrier option with an arbitrary payoff $\varphi(x)$ at maturity T (depending on the price

level x prevailing at T), given underlying dynamics (1), the natural barrier, and a price of y at time t:

$$v(y,t) = e^{-\tilde{r}(t,T)} \int_{b^\diamond(T)}^{\infty} g^+(x,T|y,t)\,\varphi(x)\,dx\,, \tag{6}$$

with the Green function g^+ defined as

$$g^+(x,T|y,t) := \begin{cases} g(x,T|y,t)\left(1-\exp\left\{-\frac{\ln\frac{b^\diamond(T)}{x}\ln\frac{b^\diamond(t)}{y}}{\tilde{\alpha}(t,T)}\right\}\right), & T>t\,, \\ 0\,, & \text{else,} \end{cases} \tag{7}$$

where

$$g(x,T|y,t) := \frac{1}{2x\sqrt{\pi\tilde{\alpha}(t,T)}}\exp\left\{-\frac{\left(\ln\frac{x}{y}+\tilde{\alpha}(t,T)-\tilde{\beta}(t,T)\right)^2}{4\tilde{\alpha}(t,T)}\right\}. \tag{8}$$

The Green function g^+ solves the Kolmogorov forward PDE and can be interpreted as a truncated state-price density reflecting the probability of the event that the barrier has not yet been touched.

To obtain the time-0 value of a defaultable zero-coupon bond in the first-hitting-time setup with asset value dynamics (1) and the natural default boundary, we set the payoff at maturity $\varphi(x) \equiv 1$ in (6):

$$\widetilde{P}(T|y_0,0) = e^{-\tilde{r}(0,T)} \int_{b^\diamond(T)}^{\infty} g^+(x,T|y_0,0)\,dx\,. \tag{9}$$

In the following we denote by $Q(T|y,t)$, $0 \le t \le T$, the survival probability of the obligor up to time T given an asset value of y at time t. Since generally $\widetilde{P}(T|y_0,0) = P(T|0)\,Q(T|y_0,0)$ under deterministic interest rates, the above expression yields a direct representation for the survival probability in case the natural default boundary is employed:

$$Q(T|y_0,0) = \int_{b^\diamond(T)}^{\infty} g^+(x,T|y_0,0)\,dx\,. \tag{10}$$

Figure 1 shows the behavior of the survival probability as the asset value at valuation time, y_0, moves away from the natural default boundary: Survival becomes more and more likely, and is eventually certain.

We are interested in a more general default boundary than the natural one and therefore sacrifice

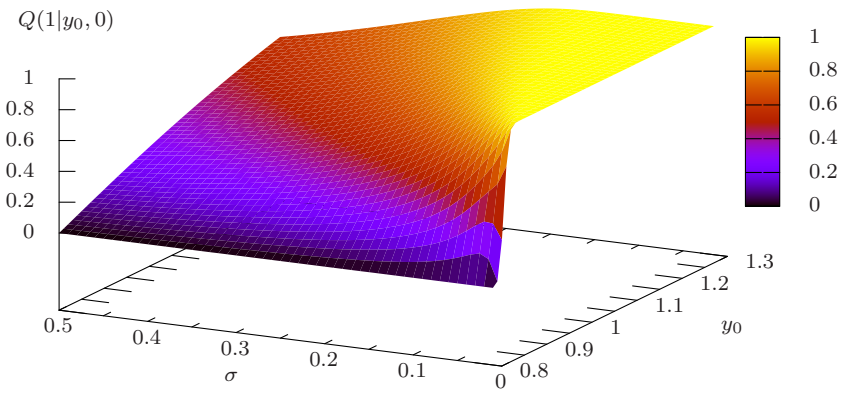

Figure 1: **Survival Probabilities Using the Natural Barrier:** The figure displays the 1-year survival probability, $Q(1|y_0, 0)$, for varying initial asset values y_0 and different asset volatilities $\sigma(t) = \sigma$ (taken constant for simplicity), given a typical parameter constellation: $q(t) = 0$, $r(t) = 3\%$, $b^\diamond(0) = 0.8$, and $b^\diamond(1) = 0.8e^r$. If $y_0 = b^\diamond(0)$, the default barrier is hit and survival probability equals zero. As y_0 increases, survival becomes more likely and survival probability approaches 1.

the closed-form solution for the survival probability which comes with the natural boundary. Instead, we assume a flexible default boundary and develop a fast and efficient numerical algorithm to approximate survival probabilities induced by this general boundary with the closed-form ones induced by the natural one. Section 3 lays out a detailed description.

2.2 CDS Pricing

There are two sides to a CDS contract: the fixed leg, comprising the fee payments by the protection buyer, and the default leg, containing the contingent payment by the protection seller. The exact cash flow structure of the fixed leg in a standardized contract is described in Appendix B.1. We assume absence of any transaction costs and other market imperfections.[3] Since we price CDS contracts at initiation only, the values of the fixed and floating legs are always at the time of initial offering, i.e. at time 0.

[3]Our valuation approach ignores the default risk of the two counterparties to a CDS contract and only accounts for the default risk of the underlying obligor. More precisely, the assumption is that during the life of the contract the counterparties either maintain the credit rating underlying generic (e.g. A-rated) CDS or have symmetric default probabilities (credit quality), cf. Duffie and Singleton (1997). We presume that this aspect has a relatively low impact on the spreads of typical CDS contracts.

Fixed Leg. Consider a CDS with outstanding premium payments at times $T_1 < T_2 < \ldots < T_N$, with $T_1 \geq T_0 = 0$ and maturity at $T = T_N$, where both premium (p.a.) and notional amounts are normalized to 1. If default happens within the protection period, the protection buyer has made $I(\tau) := \max\{0 \leq i \leq N-1 : T_i \leq \tau\}$ premium payments, the possibly remaining ones being no longer due, except for an accrued premium payment of $\tau - T_{I(\tau)}$ at the default time. Hence, the value of the fixed leg of a CDS contract initiated at time 0 with maturity T is given by

$$\begin{aligned} V^{\text{fix}}(T) &= \sum_{i=1}^{N} (T_i - T_{i-1})\, P(T_i|0)\, \mathbb{E}^{\mathbb{Q}}\left[\mathbb{1}_{\{\tau > T_i\}}\right] + \mathbb{E}^{\mathbb{Q}}\left[(\tau - T_{I(\tau)})\, P(\tau|0)\, \mathbb{1}_{\{\tau \leq T\}}\right] \\ &= \sum_{i=1}^{N} (T_i - T_{i-1})\, P(T_i|0)\, \mathbb{Q}\left[\tau > T_i\right] + \int_0^T (s - T_{I(s)})\, P(s|0)\, d\mathbb{Q}[\tau \leq s]\,. \end{aligned} \tag{11}$$

To price CDS it is therefore necessary that the complete term structure of survival probabilities is available each day. The integral above is evaluated by numerical integration. First, it is decomposed:

$$\int_0^T (s - T_{I(s)})\, P(s|0)\, d\mathbb{Q}[\tau \leq s] \;=\; \sum_{i=1}^{N} \int_{T_{i-1}}^{T_i} (s - T_{i-1})\, P(s|0)\, d\mathbb{Q}[\tau \leq s]\,. \tag{12}$$

Then, auxiliary integration points are introduced between each T_{i-1} and T_i corresponding to the chosen numerical integration rule. Using a 5-point rule, we introduce the points $T_i^1, \ldots, T_i^5$ and discretize:

$$\begin{aligned} \int_{T_{i-1}}^{T_i} (s - T_{i-1})\, P(s|0)\, d\mathbb{Q}[\tau \leq s] &= \int_{T_{i-1}}^{T_i} (s - T_{i-1})\, P(s|0)\, d(1 - \mathbb{Q}[\tau > s]) \\ &\approx -\sum_{j=1}^{6} w_j\, (T_i^j - T_{i-1})\, P(T_i^j|0)\, \frac{\mathbb{Q}[\tau > T_i^j] - \mathbb{Q}[\tau > T_i^{j-1}]}{T_i^j - T_i^{j-1}} \end{aligned} \tag{13}$$

with $T_i^0 = T_{i-1}$ and $T_i^6 = T_i$ by convention. The quadrature weights w_j are computed according to a 5-point Gauss-Legendre rule. Figure 2 depicts numerical evaluation of a typical 1-year CDS contract.

Default Leg. In principle, structural models endogenize the recovery payment at default. In the specific setting of first-passage-time models, the boundary level $b(\tau)$ at the time of default τ constitutes the natural recovery value assuming continuous asset value dynamics and a continuous boundary function.[4] Unfortunately, such an endogenous recovery formulation in our setup results in near-zero CDS premia: On the one hand, the safety barrier is calibrated too low, causing practically

[4] Various refinements of this basic idea are possible, e.g. accounting for bankruptcy costs or assuming a stationary leverage ratio as in Collin-Dufresne and Goldstein (2001).

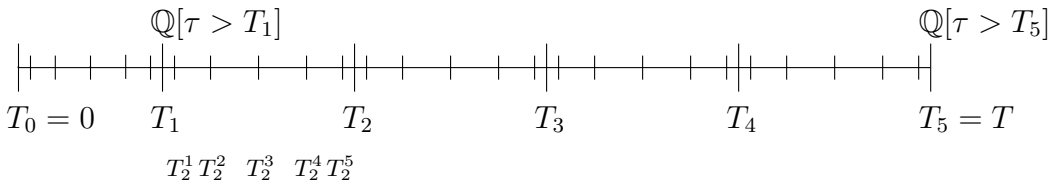

Figure 2: **Exemplary Numerical CDS Pricing:** The figure displays time segments underlying the numerical evaluation of the 1-year CDS spread using a 5-point quadrature rule. Each quarterly interval is decomposed into subsegments corresponding to the spacing in the 5-point integration rule. The time interval $[T_0, T_1]$ extends the total protection period and represents the maturity offset in case the CDS contract is *not* initiated exactly on a premium payment date.

certain survival (i.e. zero default probabilities), on the other hand it is calibrated too high compared to the face value of outstanding debt, causing zero loss in the event of default.[5]

We employ the standard recovery of face value formulation in the default-contingent leg since it coincides with the definition of the default payment in CDS, where only the notional value of the contract is protected. As other related studies (e.g. Brigo and Morini, 2006), we assume that a given constant fraction $R \in [0, 1]$ of the outstanding face value is recovered by bondholders at the default time and delivered in the CDS contract in exchange for par. The value of the default leg is thus given by

$$V^{\text{def}}(T) = \mathbb{E}^{\mathbb{Q}}\left[(1-R)\, P(\tau|0)\, \mathbb{1}_{\{\tau \le T\}}\right] = (1-R) \int_0^T P(s|0)\, d\mathbb{Q}[\tau \le s]\,. \tag{14}$$

The concrete recovery rate specified in our application (cf. Section 4) corresponds to the value recommended by Schneider et al. (2007) taking into account rating and industry affiliation of the obligor.

CDS Premium. At initiation of a CDS the premium is chosen such that the contract value to both parties is zero. Since the value of the fixed leg is homogeneous of degree 1 in the premium amount, it follows that the premium $s(T)$ on a CDS contract initiated at time 0 with maturity T equals

$$s(T) \;=\; \frac{V^{\text{def}}(T)}{V^{\text{fix}}(T)}\,. \tag{15}$$

[5] Similarly as the Merton (1974) model, first-passage-time models generally also produce spreads too close to zero for short maturities to be consistent with market data. The reason for such behavior is that the default time is predictable with respect to the natural filtration of the asset value process. The predictable-default setup used in this paper can be extended to produce inaccessible default times by allowing investors to observe only incomplete information on the asset value process and/or the default boundary. A random default barrier unobserved by investors is introduced in Giesecke and Goldberg (2004), Giesecke (2006) and Schmidt and Novikov (2008), while Brigo and Tarenghi (2005a) and Brigo and Morini (2006) suggest a scenario-dependent default barrier modeling the uncertain level of liabilities.

3 Survival Probabilities

This section explains how to approximate the survival probability $\mathbb{Q}[\tau > T]$ for any given time horizon T in case a general default boundary b is employed. Since the procedure described below is repeated for each survival probability necessary to evaluate the fixed and floating legs each time a CDS is revalued (cf. (11), (13) and (14)), it needs to be efficient and robust.

We approximate the general default boundary b using natural boundaries of the form (4). The time interval $[0, T]$ is dissected into subintervals by auxiliary time steps $0 = t_0 < t_1 < \ldots < t_n = T$, not necessarily equidistant. An approximating natural barrier $b_i^\diamond$ of the form (4) is constructed separately on each subinterval $[t_{i-1}, t_i]$, $i = 1, \ldots, n$:

$$b^\diamond(t) := \sum_{i=1}^{n} b_i^\diamond(t)\, \mathbb{1}_{[t_{i-1},t_i]}(t) \quad \text{for} \quad 0 \le t \le T\,, \tag{16}$$

with the respective start and end points, represented by the free parameters c resp. d in (4), fixed to the values of the general barrier b at the corresponding times, i.e. $b_i^\diamond(t_{i-1}) = b(t_{i-1})$ and $b_i^\diamond(t_i) = b(t_i)$:

$$b_i^\diamond(t) = \exp\left\{\frac{\tilde\alpha(t_{i-1},t_i)\,\tilde\beta(t_{i-1},t) - \tilde\alpha(t_{i-1},t)\tilde\beta(t_{i-1},t_i)}{\tilde\alpha(t_{i-1},t_i)}\right\}\left(\frac{b(t_i)}{b(t_{i-1})}\right)^{\frac{\tilde\alpha(t_{i-1},t)}{\tilde\alpha(t_{i-1},t_i)}} b(t_{i-1}) \quad \text{for} \quad t_{i-1} \le t \le t_i\,. \tag{17}$$

The questions remain how many subintervals to choose and where to place the auxiliary time steps. The approximate survival probability resulting from our method converges towards the exact value the finer the partition. This fact follows from general results on parabolic PDEs (in particular the Nagumo–Westphal lemma, cf. Walter, 1964, Section 24) as shown e.g. in Hawlitschek (1989). These theoretical results warrant asymptotic convergence, but do not provide a guideline to optimally choose a finite mesh of subintervals. We therefore develop an efficient procedure for finding dissection points which flexibly adjusts to the prespecified barrier shape. Number and position of auxiliary time steps are determined with regard to the approximation error they imply on the respective segments, cf. Proposition 2 below. Our procedure for locating them is described in Appendix B.2.

3.1 Approximation Quality

The quality of the approximation for the barrier naturally determines the quality of the approximation for the corresponding barrier hitting probabilities. The problem at hand can be reduced to resp. embedded in the more general issue of approximating probabilities of a Brownian motion hitting prespecified deterministic upper and/or lower barriers. Explicit analytic solutions to boundary crossing problems practically do not exist, except in very special cases (e.g. linear, quadratic or square-root boundaries, cf. Kahalé, 2007). Classical papers deal with smooth curved boundaries

and derive the first-passage-time density as an approximate solution to an integral or differential equation following the Kolmogorov PDE method (e.g. via a series expansion as in Ricciardi et al., 1984; Sacerdote and Tomassetti, 1996). Our setup is related to a more recent approach which approximates a possibly discontinuous barrier by a piecewise linear one (Wang and Pötzelberger, 1997) and estimates the hitting probability by Monte Carlo integration (Wang and Pötzelberger, 2001) or using numerical quadrature (Novikov et al., 1999; Borovkov and Novikov, 2005).

Proposition 1. *Let $\{y_t, t \geq 0\}$ be the asset value process modeled as a geometric Brownian motion satisfying (1). Then there exists a standard Brownian motion $\{\bar{B}_t, t \geq 0\}$ such that for an arbitrary deterministic default (i.e. lower) boundary $b(t) > 0$ with $y_0 > b(0)$ the survival probability over $[0, T]$ can be expressed as*

$$\mathbb{Q}[y_t > b(t), \forall t \in [0,T]\,] \;=\; \mathbb{Q}[\bar{B}_t > \bar{b}(t), \forall t \in [0,T]\,]\,, \tag{18}$$

where $\bar{b}$ denotes a transformed boundary of the form

$$\bar{b}(t) = \frac{1}{\sqrt{\frac{2}{t}\tilde{\alpha}(0,t)}} \ln\left(\frac{b(t)}{y_0}\, e^{\tilde{\alpha}(0,t)-\tilde{\beta}(0,t)}\right) \quad \textit{for} \quad 0 \leq t \leq T\,, \tag{19}$$

with functions $\tilde{\alpha}$ and $\tilde{\beta}$ as defined in (5).

Proof. The proof is given in Appendix A.1. □

Proposition 1 holds for an arbitrary deterministic barrier, i.e. possibly discontinuous, but one must impose certain regularity conditions to assess the approximation quality:

Proposition 2. *Let y_t be as in Proposition 1 with short rate r and dividend yield q square integrable on $[0,T]$. Further, let $b(t) > 0$ be any deterministic default boundary with $y_0 > b(0)$ such that its first derivative b' exists and is square integrable on $[0,T]$, and let $b^\diamond$ be the piecewise natural approximation (16) to boundary b given dissection points $0 = t_0 < t_1 < \ldots < t_n = T$.*

With $\bar{b}$ denoting the transform of an arbitrary boundary b derived in Proposition 1, the approximation errors are estimated as follows:

1. *for the boundary itself:*

$$|\bar{b} - \bar{b}^\diamond|_2^2 \;\leq\; \sum_{i=1}^{n} (t_i - t_{i-1})^2\, |\bar{b}' - (\bar{b}_i^\diamond)'|_2^2\,, \tag{20}$$

2. *for the survival probability over $[0,T]$:*

$$|\,\mathbb{Q}[y_t > b(t), \forall t \in [0,T]\,] - \mathbb{Q}[y_t > b^\diamond(t), \forall t \in [0,T]\,]\,| \;\leq\; \sqrt{\frac{2}{\pi}}\, |\bar{b}' - (\bar{b}^\diamond)'|_2\,, \tag{21}$$

where $|\cdot|_2$ *denotes the* L_2*-norm on the corresponding intervals.*

Proof. The error estimates are derived in Appendix A.2. □

Our procedure for locating dissection points (cf. Appendix B.2) takes into account the approximation error they imply on the respective segments: In view of Proposition 2, in the empirical application we require the approximation error $|\bar{b}' - (\bar{b}_i^{\diamond})'|_2$ on any individual subinterval $[t_{i-1}, t_i]$ of $[0, T]$ not to exceed a prespecified value ε. The overall approximation error for the survival probability can only be calculated after the dissection points are located since

$$\frac{2}{\pi}\,|\bar{b}' - (\bar{b}^{\diamond})'|_2^2 \;=\; \frac{2}{\pi}\sum_{i=1}^{n_\varepsilon} |\bar{b}' - (\bar{b}_i^{\diamond})'|_2^2 \;\leq\; \frac{2\,n_\varepsilon\,\varepsilon^2}{\pi}\,. \tag{22}$$

3.2 Computation

Next, the initial problem of calculating the overall survival probability until a certain time horizon T using the general default barrier is broken down into simpler tasks of calculating interim survival probabilities using the piecewise natural barrier. Appendix C provides a probabilistic explanation of the method. There are two slightly different steps in the iterative computation of the survival probability over $[0, T]$: computing the survival probability from time t_{n-1} to t_n and from time t_i to t_n, $i < n-1$. In both steps we exploit the fact that a probability cannot exceed 1.

Survival Probability over $[t_{n-1}, t_n]$. At time t_{n-1} the survival probability up to time t_n is available in closed form (10). On the last subinterval we are thus left with (note that $b(t_n) = b^{\diamond}(t_n)$):

$$Q(t_n|y, t_{n-1}) = \int_{b(t_n)}^{\infty} g^+(x, t_n|y, t_{n-1})\,dx\,. \tag{23}$$

Now define the integral above as a function of its lower integration boundary:

$$\mathcal{G}^+(z, t_n|y, t_{n-1}) := \int_{z}^{\infty} g^+(x, t_n|y, t_{n-1})\,dx\,. \tag{24}$$

A closed-form expression for $\mathcal{G}^+(z, t_n|y, t_{n-1})$ is derived in Appendix B.3. Since (23) represents a survival probability, the value of $Q(t_n|y, t_{n-1}) = \mathcal{G}^+(b(t_n), t_n|y, t_{n-1})$ approaches 1 the further the asset value y at time t_{n-1} lies away from the default barrier $b(t_{n-1})$, as illustrated in Figure 1. We employ the Newton-Raphson algorithm to find the asset value $y_{n-1}^{\star}$ at t_{n-1} for which $\mathcal{G}^+(b(t_n), t_n|y_{n-1}^{\star}, t_{n-1})$ is equal to 1 up to a prespecified numerical error (cf. Appendix B.4). $y_{n-1}^{\star}$ is the lowest asset value

at time t_{n-1} for which survival until t_n is (numerically) certain. This threshold value is used in the subsequent step to improve stability and efficiency.

Survival Probability over $[t_i, t_n]$. At an intermediate point in time t_i, $0 \leq i < n-1$, the survival probability until t_n given asset value y at time t_i is derived by applying the law of total probability (note that $b(t_{i+1}) = b^\diamond(t_{i+1})$):

$$Q(t_n|y,t_i) = \int_{b(t_{i+1})}^{\infty} Q(t_n|x,t_{i+1})\, g^+(x,t_{i+1}|y,t_i)\, dx\,, \tag{25}$$

which is then decomposed and approximated as

$$Q(t_n|y,t_i) \approx \int_{b(t_{i+1})}^{y^\star_{i+1}} Q(t_n|x,t_{i+1})\, g^+(x,t_{i+1}|y,t_i)\, dx + \mathcal{G}^+(y^\star_{i+1},t_{i+1}|y,t_i)\,, \tag{26}$$

knowing that $Q(t_n|x,t_{i+1})$ is essentially 1 for $x \geq y^\star_{i+1}$ (up to the prespecified numerical error). Making use of the threshold value $y^\star_{i+1}$, the survival probability $Q(t_n|y,t_i)$ can therefore be decomposed into two terms, both of which are known explicitly; neither a proxy for infinity nor a change of variables is necessary. The second integral in (26) is available in closed form (cf. Appendix B.3). The first integral is calculated using a 21-point Gauss-Legendre quadrature rule:

$$\int_{b(t_{i+1})}^{y^\star_{i+1}} Q(t_n|x,t_{i+1})\, g^+(x,t_{i+1}|y,t_i)\, dx \approx \sum_{j=1}^{21} w_j\, Q(t_n|y^j_{i+1},t_{i+1})\, g^+(y^j_{i+1},t_{i+1}|y,t_i)\,, \tag{27}$$

where the weights w_j and auxiliary points y^j_{i+1} are determined by the chosen numerical integration rule. In practice even a low-order rule yields accurate results since both survival probability and the Green function are smooth and the interval $[b(t_{i+1}), y^\star_{i+1}]$ is small. For the computation of $y^\star_i$, the threshold value for use on the next subinterval, we again employ the Newton-Raphson algorithm (cf. Appendix B.4).

Overview of the Algorithm. The following description states the algorithm in compressed form; Figure 3 illustrates. For each survival probability $\mathbb{Q}[\tau > T]$:

1. Find the time grid according to Appendix B.2, so that subintervals are defined by $0 = t_0 < t_1 < \ldots < t_n = T$. Set $y^\star_n \leftarrow b(t_n)$ and $i \leftarrow n-1$.

2. Determine $y^\star_i$ according to the Newton-Raphson algorithm from Appendix B.4.

3. Compute $Q(t_n|y_i^j, t_i)$ for y_i^j spaced on $[b(t_i), y_i^\star]$ according to a 21-point quadrature rule using approximation (26). Decrement i. Go to step 2 until $i = 1$.

4. Finally, compute the survival probability $\mathbb{Q}[\tau > T]$ as $Q(t_n|y_0, 0)$.

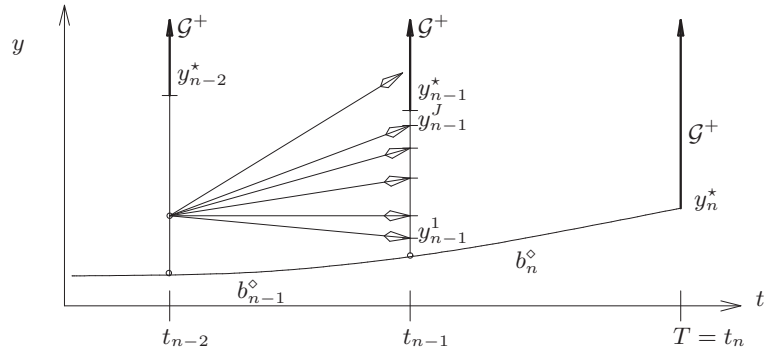

Figure 3: **Numerical Algorithm:** The figure displays how the survival probability is propagated backwards in time starting from $T = t_n$. Default barrier $b(t)$ is approximated with $b_i^\diamond(t)$ on subinterval $[t_{i-1}, t_i]$. Thick vertical arrows represent the part of the approximation (26) computed using $\mathcal{G}^+$. Thin vertical lines represent the part evaluated using numerical integration (27). Values $Q(t_n|y_{n-1}^j, t_{n-1})$, $1 \le j \le 21$, are computed by (24) as $\mathcal{G}^+(b(t_n), t_n|y_{n-1}^j, t_{n-1})$.

4 Empirical Application

4.1 Model Specification

Our approach breaks the functional dependence of the default boundary on asset volatility, short rate and dividend yield, which are treated here as exogenous inputs and calibrated to market data independently from the default model. A perfect fit to CDS quotes is accomplished by calibrating the flexible default barrier. Such a procedure represents a significant extension over the existing literature.

The functional form of the default barrier in Hui et al. (2003) and Brigo and Tarenghi (2005b) is completely determined by the instantaneous short rate, dividend yield, and the instantaneous asset volatility. In the latter paper, CDS quotes are fitted by adjusting the steps of a piecewise constant instantaneous volatility function. The procedure is tested on several trading days preceding the default of *Parmalat SpA*. Since the shape of the boundary is allowed to change only through the volatility function, it does not have enough freedom to reflect new information about the state of the company. Moreover, the fitted volatility parameters exhibit peculiar behavior in order to match market CDS quotes, and especially the volatility obtained in the short term appears rather high.

In our setup, the functional forms for $\sigma^2(t)$, $r(t)$ and $q(t)$ can be freely chosen. We set $q(t) \equiv 0$ and choose the Nelson-Siegel function (cf. Nelson and Siegel, 1987) for the short rate and the asset volatility since this form is reasonably flexible, yet easily integrable:

$$r(t) = c_0 + c_1 \exp\left(-\frac{t}{\tau_r}\right) + c_2 \frac{t}{\tau_r} \exp\left(-\frac{t}{\tau_r}\right), \tag{28}$$

and

$$\sigma^2(t) = d_0 + d_1 \exp\left(-\frac{t}{\tau_s}\right) + d_2 \frac{t}{\tau_s} \exp\left(-\frac{t}{\tau_s}\right). \tag{29}$$

By integrating over the formulas above we obtain (observable) zero-bond yields $z(t)$:

$$z(t) = \frac{1}{t}\int_0^t r(s)\,ds = c_0 + (c_1 + c_2)\left(1 - \exp\left(-\frac{t}{\tau_r}\right)\right)\frac{\tau_r}{t} - c_2 \exp\left(-\frac{t}{\tau_r}\right), \tag{30}$$

and asset variances $\varsigma_y^2(t)$:

$$\varsigma_y^2(t) = \frac{1}{t}\int_0^t \sigma^2(s)\,ds = d_0 + (d_1 + d_2)\left(1 - \exp\left(-\frac{t}{\tau_s}\right)\right)\frac{\tau_s}{t} - d_2 \exp\left(-\frac{t}{\tau_s}\right). \tag{31}$$

Riskless zero-bond yields are bootstrapped from euro-denominated swap rates, which are available on a daily basis for standard maturities between 1 and 12 years (1, 1.5, 2, 2.5, and 3 to 12 years). For maturities shorter than one year we use money-market (Euribor) rates with monthly maturities. All riskless data is obtained from Bloomberg.

Since the asset value y_t cannot be directly observed, one resorts to estimating the coefficients of its dynamics (1), in particular the volatility function, from observed equity data. Earlier studies, such as Eom et al. (2004), infer only a constant volatility parameter either from historical equity prices or from implied bond volatilities. In this study, asset volatility $\varsigma_y(t)$ is a deterministic function of time, and we derive it from option-implied equity volatilities. A straightforward calculation of $\varsigma_y(t)$ is suggested in Lando (2004, p. 42 et seq.): If the leverage ratio d_0/e_0, relating current market value of debt d_0 to current market value of equity e_0, is low, asset volatility can be approximated by

$$\varsigma_y(t) \approx \frac{e_0}{y_0}\,\varsigma_e(t)\,, \tag{32}$$

where $\varsigma_e(t)$ denotes the option-implied equity volatility for time horizon t. The ratio e_0/y_0 of current equity to asset value is expressed as

$$\frac{e_0}{y_0} = \frac{e_0}{d_0 + e_0} = \frac{1}{1 + d_0/e_0}\,, \tag{33}$$

where the leverage ratio is approximated by the ratio of face value of debt to market value of equity, using the ratio of total liabilities to equity published quarterly in Bloomberg.[6] For shorter maturities between 10 days and 2 years, we take the mean of the put- and call-implied equity volatility (implied from at-the-money put and call options). To estimate the unconditional long-term equity volatility we employ the daily implied volatility calculated from a weighted average of the volatilities of the three call options closest to the at-the-money strike, averaging the daily values over the two years preceding the respective observation periods. All volatilities are also published by Bloomberg. The coefficients are fitted to market data by a combination of OLS and a grid search for τ_r resp. τ_s as described in the original paper (cf. Nelson and Siegel, 1987).

Calibration of the model to CDS premia is accomplished by the flexible shape of the default barrier. In order to exactly calibrate the cross section of CDS maturities on a given day, we specify the default boundary as follows:

$$b(t;a) = \begin{cases} a_0, & 0 \le t \le M_1, \\ a_0 + a_1(t-M_1)^2, & M_1 < t \le M_3, \\ a_0 + 4a_1 + 4a_1(t-M_3) + a_2(t-M_3)^2, & M_3 < t \le M_5, \\ a_0 + 12a_1 + 4a_2 + 4(a_1+a_2)(t-M_5) + a_3(t-M_5)^2, & M_5 < t \le M_7, \\ a_0 + 20a_1 + 12a_2 + 4a_3 + 4(a_1+a_2+a_3)(t-M_7) + a_4(t-M_7)^2, & M_7 < t \le M_{10}. \end{cases} \tag{34}$$

where $a = (a_0, \ldots, a_4) \in \mathbb{R}^5$ denotes the parameter vector, and M_n the maturity date of the n-year CDS contract. We take into account only the five canonical CDS maturities (cf. Brigo and Mercurio, 2006, p. 719) of 1 year, 3 years, 5 years, 7 years, and 10 years since these are most frequently quoted and traded. The segments of the piecewise quadratic default boundary (34) satisfy value-matching and smooth-pasting conditions, making the boundary continuously differentiable and thus satisfying the necessary conditions for the numerical procedure. It turns out that the typical subintervals resulting from our dissection algorithm are possibly large (several years), but still with only small deviations between b and its natural approximation $b^\diamond$, as Figure 4 illustrates. CDS premia are fitted one after the other, starting with the shortest maturity, by varying each of the parameters a_0 to a_4 in turn until the respective model-implied CDS premium agrees with its observed market premium. Implemented in C++, calibration on a cross section of CDS premia for a single day takes 0.1-1 seconds depending on the initial guess for the default barrier.

[6] More precisely, the Bloomberg item for the debt-to-market-cap ratio is used, which is calculated as the sum of short-term and long-term debt over market capitalization.

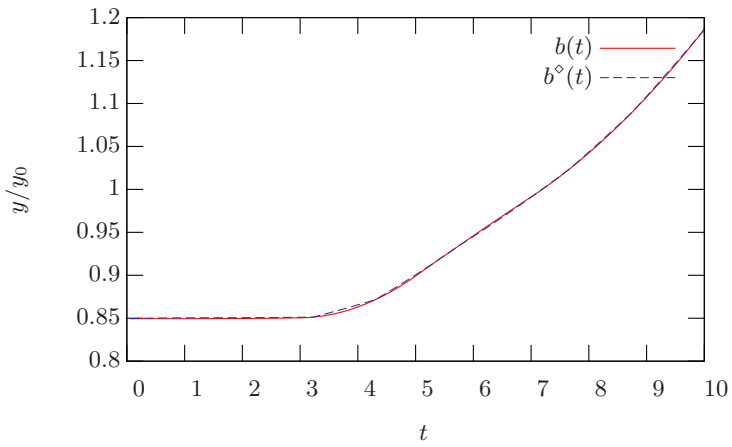

Figure 4: **Barrier Approximation:** The figure displays the default barrier $b(t)$ from (34) estimated using actual data for *Daimler Chrysler AG* on the first day in our sample, along with its piecewise natural approximation $b^\diamond(t)$ over a 10-year period. Condition $|\bar{b}' - (\bar{b}_i^\diamond)'|_2 \leq \varepsilon$ yields five discretization points.

4.2 Results

We take our model to market data using panels of EUR-denominated CDS with the Modified Modified Restructuring clause written on senior unsecured debt of *Telecom Italia SpA* (TIT) and *Daimler Chrysler AG* (DCX). CDS history is obtained from Markit, a leading data provider specializing in mark-to-market CDS pricing. Both samples start on May 6$^{\text{th}}$, 2005 and end on October 31$^{\text{st}}$, 2006. The two obligors are reported to be investment-grade, rated BBB during the entire observation period. Industry affiliation according to the ICB scheme is *Consumer Goods* for DCX and *Telecommunications* for TIT. The recovery parameter is set to 63% for DCX and 76% for TIT, as recommended in Schneider et al. (2007).

Figures 6 and 7 show input data as well as results of the calibration for each of the two obligors: The upper panels depict the default barrier and survival probabilities under $\mathbb{Q}$ implied by the cross section of CDS spreads, leverage (here debt-to-equity) ratios, and asset volatilities, all shown in the lower panels. The lines plotted in Panels 6a/7a, 6b/7b and 6c/7c represent vertical sections of the corresponding surfaces at maturities of 1, 3, 5, 7 and 10 years. For the default barriers to be comparable Panels 6a/7a show their transform as derived in Proposition 1, meaning that they now relate to standard (arithmetic) Brownian motion. By accounting for riskless compounding the transform essentially[7] represents the ratio of the original barrier level $b(t)$ to the expected asset level at the corresponding point in time $\mathbb{E}[y_t]$, normalized by asset volatility. The implied barrier functions (in the cross section of maturities) on consecutive days during the time period considered

[7] Up to the logarithm, which transforms a geometric barrier into an arithmetic one.

are similar in shape for both obligors (not displayed); changes in the default boundary over time are thus small, indicating in particular that our method produces stable output.

For a full understanding one must keep in mind the causal relationships between the individual model elements: Riskless interest rates (not displayed) and asset volatility affect the profile of the resulting default barrier. Basic inputs to asset volatility are option-implied equity volatility (not displayed) and firm leverage ratio, which determine asset volatility according to (32). Statements about the default barrier must therefore take all three underlying quantities into account – interest rate, leverage, and equity volatility. We concentrate here on the latter two.

Option-implied equity volatility lies in the common range between 20 and 30 percent (both across maturities and in calendar time) for both obligors, and scarcely exhibits excessive behavior. The DCX debt-to-assets ratio first falls by around 7% to 63%, remains approximately stable for nine months (due to quarterly data publishing), and then rises by around 5%. TIT shows a fairly stable capital structure with debt-to-assets much less volatile and changing only within a 3% range, compared to an 8% range for DCX. Panels 6c/7c and 6d/7d show that shifts in implied asset volatility can mostly be attributed to changes in firm leverage, here especially pronounced for DCX. Moreover, asset volatility is affected by leverage more pronouncedly in the long term (5, 7 and especially 10 years), while short-term asset volatility rather reflects fluctuations in short-term equity volatility.

As expected, movements in CDS spreads (resp. implied survival probabilities) have a dominant effect on the transformed default barrier both in the short and long term, which is seen by comparing the behavior in time of CDS spread Panels 6d/7d (resp. survival probabilities in Panels 6b/7b) and the barrier sections in Panels 6a/7a for individual maturities. The asset volatility has an effect on the default barrier as well since volatility peaks show up in the default barrier. As transformed barriers may be compared between obligors, we observe that the market deems TIT to be increasingly more default-prone in the long run than DCX, while their short-term levels are similar. Such a differentiated observation would not be possible merely by looking at CDS spreads.

Level and slope of the default barrier are related to market perceptions of changes in the future financial situation of an obligor. The default barriers implied by both CDS panels exhibit a downward hump at a maturity of approximately 5 years and are convexly upward sloping for longer maturities. The downward hump shape indicates that the boundary structure employed in e.g. Brigo and Morini (2006), implying exponential growth, is not satisfactory and could possibly turn out misleading when describing the term structure of market expectations. The calibration of the boundary in the previously cited papers (cf. Section 4.1) is performed over the term structure of asset volatilities, so that the volatility values implied from CDS premia must absorb the variability of CDS-implied (conditional) survival probabilities in the maturity dimension, and thus yield the less intuitive asset volatility patterns reported in these studies.

Finally, Figure 5 shows survival probabilities under the physical measure $\mathbb{P}$ arising with different

estimates for the asset drift under $\mathbb{P}$. The cross section of CDS maturities observed on the first day in our sample underlies the figure. As intuitively expected, the survival probability curve (in the maturity cross section) is steeply decreasing for low values of the asset drift (down to roughly 60% at 10 years), and gradually flattens out almost into a straight line at 1 for values of the drift higher than approximately 8%. Given that both obligors have an S&P rating of BBB on this day we can compare the survival probabilities under $\mathbb{P}$ above with typical values which S&P associates with a BBB rating.[8] For both obligors the distance between S&P's and our survival probabilities is smallest at asset drifts of 6 to 7 percent. The opposite direction is also conceivable: In case the matrix of default probabilities provided by rating agencies is too coarse for a given task, default probabilities can be computed from our model using a given estimate of asset growth to achieve a refined view of default probabilities.

5 Conclusion

We introduce a generalized Black&Cox-type structural model for credit default swaps in which the default barrier is allowed to vary freely with the term. The model extends earlier work by e.g. Brigo and Morini (2006), who choose a specific form for the default barrier for tractability. With exogenous estimates for asset volatility, dividend yield and interest rates, the default barrier is calibrated such that a given maturity cross section of CDS contracts is perfectly fitted. We develop a refined and computationally efficient numerical method with attractive numerical stability.

We take our model to market data and apply it exemplarily to CDS contracts written on *Telecom Italia SpA* and *Daimler Chrysler AG*. The results show that the barrier shape employed in previous papers is not satisfactory and could possibly turn out misleading when describing the term structure of market expectations. The reason is that the boundary takes on humped shapes as well, implying slower growth in conditional default probabilities over certain periods.

Several applications of both practical and academic interest arise naturally with our model. Survival probabilities computed within our framework reflect information contained in equity volatility, interest rates, CDS premia, and capital structure. They are therefore particularly suitable for empirical studies and valuation concerning equity and default risk at the same time. Finally, the analytic framework together with the numerical algorithm developed in this paper can be extended to accommodate optimal-control problems, such as the determination of optimal debt covenants or endogenous refinancing times.

[8] The values are obtained from Vazza et al. (2007).

References

Aunon-Nerin, D., Cossin, D., Hricko, T., and Huang, Z. (2002). Exploring for the determinants of credit risk in credit default swap transaction data: Is fixed-income markets' information sufficient to evaluate credit risk? FAME Research Paper No. 65.

Benkert, C. (2004). Explaining credit default swap premia. *Journal of Futures Markets*, 24(1):71–92.

Berndt, A., Douglas, R., Duffie, D., Ferguson, M., and Schranz, D. (2008). Measuring default risk premia form default swap rates and EDFs. Working paper, Stanford University.

Black, F. and Cox, J. (1976). Valuing corporate securities: Some effects of bond indenture provisions. *Journal of Finance*, 31:351–367.

Borovkov, K. and Novikov, A. (2005). Explicit bounds for approximation rates of boundary crossing probabilities for the Wiener process. *Journal of Applied Probability*, 42(1):82–92.

Brigo, D. and Masetti, M. (2005). *Risk neutral pricing of counterparty risk*, chapter 10. In Pykhtin (2005).

Brigo, D. and Mercurio, F. (2006). *Interest Rate Models – Theory and Practice. With Smile, Inflation and Credit*. Springer Finance. Springer-Verlag, 2nd edition.

Brigo, D. and Morini, M. (2006). Structural credit calibration. *Risk Magazine*, April issue:78–83.

Brigo, D. and Tarenghi, M. (2005a). Credit default swap calibration and counterparty risk valuation with a scenario based first passage model. Working paper, www.damianobrigo.it.

Brigo, D. and Tarenghi, M. (2005b). Credit default swap calibration and equity swap valuation under counterparty risk with a tractable structural model. Working paper, www.damianobrigo.it.

Briys, E. and de Varenne, F. (1997). Valuing risky fixed rate debt: An extension. *Journal of Financial and Quantitative Analysis*, 32(2):239–248.

Collin-Dufresne, P. and Goldstein, R. (2001). Do credit spreads reflect stationary leverage ratios? *Journal of Finance*, 56(5):1929–1957.

Cox, D. and Miller, H. (1965). *The Theory of Stochastic Processes*. Chapman & Hall.

Dangl, T. and Zechner, J. (2004). Credit risk and dynamic capital structure choice. *Journal of Financial Intermediation*, 13:183–204.

Detemple, J. and Tian, W. (2007). Debt with endogenous safety covenants: Default and corporate securities valuation. Working paper, Boston University and University of Waterloo.

Dorfleitner, G., Schneider, P., Hawlitschek, K., and Buch, A. (2008). Pricing options with Green's functions when volatility, interest rate and barriers depend on time. *Quantitative Finance*, 8(2):119–133.

Duffie, D. and Singleton, K. (1997). An econometric model of the term structure of interest rate swap yields. *Journal of Finance*, 52(4):1287–1323.

Eom, Y. H., Helwege, J., and Huang, J.-Z. (2004). Structural models of corporate bond pricing: An empirical analysis. *Review of Financial Studies*, 17(2):499–544.

Ericsson, J., Jacobs, K., and Oviedo, R. A. (2007). The determinants of credit default swap premia. *Journal of Financial and Quantitative Analysis*. Forthcoming.

Giesecke, K. (2006). Default and information. *Journal of Economic Dynamics and Control*, 30(11):2281–2303.

Giesecke, K. and Goldberg, L. R. (2004). Forecasting default in the face of uncertainty. *Journal of Derivatives*, 12(1):11–25.

Hawlitschek, K. (1989). Approximation Greenscher Funktionen bei parabolischen Differenzialgleichungen. *Journal of Applied Mathematics and Physics (ZAMP)*, 40:912–919.

Hilberink, B. and Rogers, L. (2002). Optimal capital structure and endogenous default. *Finance and Stochastics*, 6(2):237–263.

Hsu, J. C., Saá-Requejo, J., and Santa-Clara, P. (2002). Bond pricing with default risk. Working paper, Anderson School, UCLA.

Hui, C.-H., Lo, C.-F., and Tsang, S.-W. (2003). Pricing corporate bonds with dynamic default barriers. *Journal of Risk*, 5(3):17–37.

Kahalé, N. (2007). Analytic crossing probabilities for certain barriers by Brownian motion. Working paper, ESCP-EAP.

Kim, I., Ramaswamy, K., and Sundaresan, S. (1993). The valuation of corporate fixed income securities. Working paper, Wharton School, University of Pennsylvania.

Lando, D. (2004). *Credit Risk Modeling: Theory and Applications*. Princeton University Press.

Lo, C.-F., Lee, H. C., and Hui, C.-H. (2003). A simple approach for pricing barrier options with time-dependent parameters. *Quantitative Finance*, 3(2):98–107.

Longstaff, F. A. and Schwartz, E. (1995). A simple approach to valuing risky fixed and floating rate debt. *Journal of Finance*, 50(3):789–819.

Merton, R. (1974). On the pricing of corporate debt: The risk structure of interest rates. *Journal of Finance*, 29:449–470.

Nelson, C. R. and Siegel, A. F. (1987). Parsimonious modeling of yield curves. *Journal of Business*, 60(4):473–489.

Novikov, A., Frishling, V., and Kordzakhia, N. (1999). Approximations of boundary crossing probabilities for a Brownian motion. *Journal of Applied Probability*, 36(4):1019–1030.

Pötzelberger, K. (2008). Estimating boundary crossing probabilities for diffusion processes by adaptive control variables. Working paper, Vienna University of Economics and Business Administration.

Pykhtin, M., editor (2005). *Counterparty Credit Risk Modeling: Risk Management, Pricing and Regulation*. Risk Books, Incisive Media plc.

Rapisarda, F. (2003). Pricing barriers on underlyings with time-dependent parameters. Working paper, http://it.geocities.com/rapix/TimeDependentBarriers.pdf.

Ricciardi, L. M., Sacerdote, L., and Sato, S. (1984). On an integral equation for first-passage-time probability densities. *Journal of Applied Probability*, 21(2):302–314.

Sacerdote, L. and Tomassetti, F. (1996). On evaluations and asymptotic approximations of first-passage-time probabilities. *Advances in Applied Probability*, 28(1):270–284.

Schmidt, T. and Novikov, A. (2008). A structural model with unobserved default boundary. *Applied Mathematical Finance*, 15(2):183–203.

Schneider, P., Sögner, L., and Veža, T. (2007). The economic role of jumps and recovery rates in the market for corporate default risk. Working paper, Vienna University of Economics and Business Administration.

Vazza, D., Aurora, D., Kraemer, N., Kesh, S., and Torres, J. (2007). Annual 2006 global corporate default study and ratings transitions. Technical report, Standard and Poor's, Global Fixed Income Research, New York.

Walter, W. (1964). *Differential- und Integral-Ungleichungen*. Springer-Verlag.

Wang, L. and Pötzelberger, K. (1997). Boundary crossing probability for Brownian motion and general boundaries. *Journal of Applied Probability*, 34(1):54–65.

Wang, L. and Pötzelberger, K. (2001). Boundary crossing probability for Brownian motion. *Journal of Applied Probability*, 38(1):152–164.

Wang, L. and Pötzelberger, K. (2007). Crossing probabilities for diffusion processes with piecewise continuous boundaries. *Methodology and Computing in Applied Probability*, 9(1):21–40.

Appendix

A Proofs

A.1 Proof of Proposition 1

An application of Itô's formula yields the following dynamics for the process $x_t := \ln y_t$:

$$dx_t = \left(r(t) - q(t) - \frac{\sigma^2(t)}{2} \right) dt + \sigma(t)\, dB_t \,. \tag{35}$$

By the scaling property of Brownian motion we further obtain:

$$\int_0^t \sigma(s)\, dB_s \;\stackrel{\mathcal{D}}{=}\; \left(\frac{1}{t} \int_0^t \sigma^2(s)\, ds \right)^{1/2} \bar{B}_t \,. \tag{36}$$

The survival probability in (18) thus equals:

$$\begin{aligned} \mathbb{Q}[y_t > b(t), \forall t \in [0,T]\,] &= \mathbb{Q}[x_t > \ln b(t), \forall t \in [0,T]\,] \qquad (37)\\ &= \mathbb{Q}\left[\int_0^t \sigma(s)\, dB_s > \ln \frac{b(t)}{y_0} - \int_0^t \left(r(s) - q(s) - \frac{\sigma^2(s)}{2} \right) ds, \forall t \in [0,T] \right] \\ &= \mathbb{Q}\left[\left(\frac{1}{t} \int_0^t \sigma^2(s)\, ds \right)^{1/2} \bar{B}_t > \ln \frac{b(t)}{y_0} - \tilde{\beta}(0,t) + \tilde{\alpha}(0,t), \forall t \in [0,T] \right] , \end{aligned}$$

which yields the stated default boundary $\bar{b}$ for a standard Brownian motion $\bar{B}$ (cp. Wang and Pötzelberger, 2007).

A.2 Proof of Proposition 2

1. From the piecewise definition of the approximating barrier (16) it follows that

$$|\bar{b} - \bar{b}^{\diamond}|_2^2 \;=\; \int_0^T (\bar{b}(t) - \bar{b}^{\diamond}(t))^2 dt \;=\; \sum_{i=1}^{n} \int_{t_{i-1}}^{t_i} (\bar{b}(t) - \bar{b}_i^{\diamond}(t))^2 dt \;=\; \sum_{i=1}^{n} |\bar{b} - \bar{b}_i^{\diamond}|_2^2 \,. \tag{38}$$

   Now define $f_i := \bar{b} - \bar{b}_i^{\diamond}$ on each subinterval $[t_{i-1}, t_i], i = 1, \ldots, n$. Boundary b is differentiable by assumption, while the natural boundary $b_i^{\diamond}$ is differentiable being a composite of differentiable functions. Hence, each f_i can be expressed as $f_i(t) = f_i(t_{i-1}) + \int_{t_{i-1}}^t f_i'(s) ds$ for $t_{i-1} \le t \le t_i$. Since $f(t_{i-1}) = f(t_i) = 0$ by construction, we obtain:

$$|f_i(t)| \;\le\; \int_{t_{i-1}}^t |f_i'(s)| ds \;\le\; \int_{t_{i-1}}^{t_i} |f_i'(s)| ds \;=\; |f_i'|_1 \;\le\; \sqrt{t_i - t_{i-1}}\, |f_i'|_2 \,. \tag{39}$$

The last relation holds by the Hölder inequality since the first derivatives of both b and $b_i^\diamond$ are square integrable: b' again by assumption and $(b_i^\diamond)'$ because r and q are additionally assumed square integrable. Integrating the squared expressions over $[t_{i-1}, t_i]$ yields:

$$|\bar{b} - \bar{b}_i^\diamond|_2^2 \;=\; \int_{t_{i-1}}^{t_i} |f_i(t)|^2 dt \;\leq\; (t_i - t_{i-1})\, |f_i'|_2^2 \int_{t_{i-1}}^{t_i} dt \;=\; (t_i - t_{i-1})^2\, |\bar{b}' - (\bar{b}_i^\diamond)'|_2^2 \,. \tag{40}$$

Inserting this expression into (38) results in the stated error estimate (20).

2. Proposition 1 reduces the problem to one concerning a standard Brownian motion:

$$\begin{aligned} &|\,\mathbb{Q}[y_t > b(t), \forall t \in [0,T]\,] - \mathbb{Q}[y_t > b^\diamond(t), \forall t \in [0,T]\,]\,| \\ &\qquad = \;|\,\mathbb{Q}[\bar{B}_t > \bar{b}(t), \forall t \in [0,T]\,] - \mathbb{Q}[\bar{B}_t > \bar{b}^\diamond(t), \forall t \in [0,T]\,]\,| \,. \end{aligned} \tag{41}$$

Next apply Theorem 2 from Pötzelberger (2008) about the error in estimation when approximating a boundary in L_2-norm to obtain the stated error estimate:

$$|\,\mathbb{Q}[\bar{B}_t > \bar{b}(t), \forall t \in [0,T]\,] - \mathbb{Q}[\bar{B}_t > \bar{b}^\diamond(t), \forall t \in [0,T]\,]\,| \;\leq\; \sqrt{\frac{2}{\pi}}\, |\bar{b}' - (\bar{b}^\diamond)'|_2 \,. \tag{42}$$

B Technical Details

B.1 CDS Cash Flow Structure

The exact cash flow structure of the fixed leg in a standard contract, as laid down in the 2003 ISDA Credit Derivatives Definitions, is specified as follows: Premium payment dates are fixed and do not depend on the specific contract date. Payments are made quarterly on the 20$^{\text{th}}$ of March, June, September and December. Thus, if a CDS is contracted between those dates, the first period is not a full quarter and the first premium payment is adjusted accordingly. In addition, we account for the variable maturity of CDS contracts: As a result of fixing the premium payment dates, the length of the protection period varies and depends on the contract date since the quoted CDS maturity begins on the first premium payment date. Furthermore, the accrued premium in case of default must be taken into account. The day-count convention used in CDS contracts is *actual/360.*

B.2 Dissection Algorithm

Number and position of auxiliary time steps $\{t_i, i = 1, \ldots n-1\}$ in the approximating natural barrier $b^\diamond$ from (16) is determined with regard to the approximation error they imply on the respective segments. In view of Proposition 2, in the numerical application we require the approximation error

on any individual subinterval $[t_{i-1}, t_i]$ of $[0, T]$ not to exceed a prespecified value $\varepsilon = 0.04$:

$$|\bar{b}' - (\bar{b}_i^{\diamond})'|_2 \;\leq\; \varepsilon\,. \tag{43}$$

Since we prefer to use as few as possible dissection points, they are located such that condition (43) exactly holds on each subinterval using the following procedure: Start at the right end of the interval $[0, T]$. Keep T fixed as the upper subinterval bound and determine the lower subinterval bound t through

$$\int_t^T \left(\bar{b}'(s) - (\bar{b}_n^{\diamond})'(s)\right)^2 \, ds \;=\; \varepsilon^2\,. \tag{44}$$

In each subsequent step the upper bound of the next subinterval is fixed to the previously found lower bound of the preceding subinterval. The next lower bound is then determined by applying criterion (44). The algorithm terminates as soon as the subinterval having 0 as lower bound satisfies condition (43).

In each step equation (44) is solved using the Newton-Raphson method with objective function

$$f_i(t) := \int_t^{t_i} \left(\bar{b}'(s) - (\bar{b}_i^{\diamond})'(s)\right)^2 \, ds\,, \tag{45}$$

which is monotonically decreasing on $[0, t_i]$ with first derivative $f_i'(t) = -(\bar{b}'(t) - (\bar{b}_i^{\diamond})'(t))^2 \;\leq\; 0$:

$$t^{(0)} = t_i \qquad \text{and} \qquad t^{(k)} \;=\; t^{(k-1)} - \frac{f_i(t^{(k-1)})}{f_i'(t^{(k-1)})} \quad \text{for} \quad k \geq 1 \tag{46}$$

until $|f_i(t^{(k)}) - \varepsilon^2| < \delta = 10^{-5}$.

B.3 Function $\mathcal{G}^+$ in Closed Form

Let $t_{i-1} < t_i$ be arbitrary points in time defining subinterval $[t_{i-1}, t_i]$ with natural default barrier $b_i^{\diamond}(t)$ according to (17). Let furthermore $z, y > b(t_{i-1})$. We abbreviate $\tilde{\alpha}(t_{i-1}, t_i)$ by $\tilde{\alpha}$ and $\tilde{\beta}(t_{i-1}, t_i)$ by $\tilde{\beta}$ in the following. Φ denotes the standard normal distribution function.

$$
\begin{aligned}
\mathcal{G}^+(z,t_i|y,t_{i-1}) &:= \int_z^\infty g^+(x,t_i|y,t_{i-1})\,dx \\
&= \int_z^\infty \left(1-\exp\left\{-\frac{\ln\frac{b(t_i)}{x}\ln\frac{b(t_{i-1})}{y}}{\tilde\alpha}\right\}\right)\frac{1}{2x\sqrt{\pi\tilde\alpha}}\exp\left\{-\frac{\left(\ln\frac{x}{y}+\tilde\alpha-\tilde\beta\right)^2}{4\tilde\alpha}\right\}dx \\
&= \Phi\left(\frac{\ln\frac{y}{z}-\tilde\alpha+\tilde\beta}{\sqrt{2\tilde\alpha}}\right)-\int_z^\infty \frac{1}{2x\sqrt{\pi\tilde\alpha}}\exp\left\{-\frac{4\ln\frac{b(t_i)}{x}\ln\frac{b(t_{i-1})}{y}+\left(\ln\frac{x}{y}+\tilde\alpha-\tilde\beta\right)^2}{4\tilde\alpha}\right\}dx \\
&= \Phi\left(\frac{\ln\frac{y}{z}-\tilde\alpha+\tilde\beta}{\sqrt{2\tilde\alpha}}\right)-\int_z^\infty \frac{1}{2x\sqrt{\pi\tilde\alpha}}\exp\left\{-\frac{4\ln\frac{b(t_{i-1})}{y}\left(\ln\frac{b(t_i)}{b(t_{i-1})}+\tilde\alpha-\tilde\beta\right)+\left(\ln\frac{xy}{b(t_{i-1})^2}+\tilde\alpha-\tilde\beta\right)^2}{4\tilde\alpha}\right\}dx \\
&= \Phi\left(\frac{\ln\frac{y}{z}-\tilde\alpha+\tilde\beta}{\sqrt{2\tilde\alpha}}\right)-\exp\left(-\frac{\ln\frac{b(t_{i-1})}{y}\left(\ln\frac{b(t_i)}{b(t_{i-1})}+\tilde\alpha-\tilde\beta\right)}{\tilde\alpha}\right)\Phi\left(\frac{\ln\frac{b(t_{i-1})^2}{zy}-\tilde\alpha+\tilde\beta}{\sqrt{2\tilde\alpha}}\right). \qquad (47)
\end{aligned}
$$

B.4 Determining the Cutoff Asset Value

Both cases are solved using the Newton-Raphson method:

Survival Probability over the Last Subinterval. Starting from $y^{(0)} = b(t_{n-1})$ iterate

$$
y^{(k)} \;=\; y^{(k-1)} - \frac{\mathcal{G}^+(b(t_n),t_n|y^{(k-1)},t_{n-1})-1}{\dfrac{\partial\,\mathcal{G}^+(b(t_n),t_n|y^{(k-1)},t_{n-1})}{\partial\,y^{(k-1)}}} \quad \text{for} \quad k\geq 1 \qquad (48)
$$

until $|\mathcal{G}^+(b(t_n),t_n|y^{(k)},t_{n-1})-1| < \delta = 10^{-5}$.

Survival Probability over an Intermediate Subinterval. Starting from $y^{(0)} = b(t_{i-1})$ iterate

$$
y^{(k)} \;=\; y^{(k-1)} - \frac{Q(t_n|y^{(k-1)},t_i)-1}{\dfrac{\partial\,Q(t_n|y^{(k-1)},t_i)}{\partial\,y^{(k-1)}}} \quad \text{for} \quad k\geq 1 \qquad (49)
$$

until $|Q(t_n|y^{(k)}, t_i) - 1| < \delta = 10^{-5}$. The probability $Q(t_n|y, t_i)$ is given by (26) and (27), and therefore

$$\frac{\partial\, Q(t_n|y,t_i)}{\partial\, y} = \sum_{j=1}^{J} w_j\, Q(t_n|y_{i+1}^j, t_{i+1}) \frac{\partial\, g^+(y_{i+1}^j, t_{i+1}|y,t_i)}{\partial\, y} + \frac{\partial\, \mathcal{G}^+(y_{i+1}^\star, t_{i+1}|y,t_i)}{\partial\, y}. \tag{50}$$

The derivative of $\mathcal{G}^+$ as well as g^+ with respect to y can be computed by a symbolic mathematics package in closed form up to the Gaussian error function.

C Survival Probabilities with the Stripe Method

This section interprets the numerical computation of the survival probability (10) in probabilistic terms. It is intended to build an intuitive understanding of the PDE-related representation (10).

Let b be a continuous and piecewise differentiable default barrier. The survival probability up to time T (under the pricing measure $\mathbb{Q}$) is defined as

$$Q(T|y_0, 0) := \mathbb{Q}[y_t > b(t), \forall t \in [0, T]\,]\,. \tag{51}$$

For a barrier of the natural form (4) there exists a closed-form solution to the survival probability (10). In our application though, the barrier does not necessarily follow (4) but is an arbitrary function of time. To obtain a numerical solution we therefore employ the stripe method described in Section 3: Auxiliary time steps $0 = t_0 < t_1 < \ldots < t_n = T$ define subintervals on which the general barrier is approximated by piecewise natural barriers. The probabilistic interpretation proceeds in three steps:

I Local solution for barrier $b_i^\diamond$. Let $b_i^\diamond$ be defined as in (17). Following Cox and Miller (1965, Section 5.6) and Dorfleitner et al. (2008, Proof of Theorem 1), we see that $g^+(x, t_i|y, t_{i-1})$ fulfills the corresponding Kolmogorov forward equation with boundary conditions

$$g^+(x, t_{i-1}|y, t_{i-1}) = \delta_y(x) \quad \text{and} \quad g^+(b_i^\diamond(t), t|y, t_{i-1}) = 0 \ \text{ for } t \in (t_{i-1}, t_i) \tag{52}$$

and is thus the transition density from time t_{i-1} to t_i with starting point $y_{t_{i-1}}$. Therefore it follows that

$$\mathbb{Q}[y_t > b_i^\diamond(t), \forall t \in [t_{i-1}, t_i]\,|\, y_{t_{i-1}} = y] = \int_{b(t_i)}^{\infty} g^+(x, t_i|y, t_{i-1})\, dx\,. \tag{53}$$

This equation provides the time-t_{i-1} $\mathbb{Q}$-measure survival probability up to time t_i conditioned

on an asset value of y at time t_{i-1} if the actual barrier b is replaced by the natural barrier $b_i^\diamond$ on $[t_{i-1}, t_i]$.

II Global solution for barrier $b^\diamond$. We next show that the exact $\mathbb{Q}$-measure survival probability up to time T with respect to $b^\diamond$ is given by

$$\mathbb{Q}[y_t > b^\diamond(t),\ 0 \le t \le T] = \int_{b(t_n)}^{\infty} \dots \int_{b(t_1)}^{\infty} \prod_{i=0}^{n-1} g^+(x_{i+1}, t_{i+1}|x_i, t_i)\, dx_1 \dots dx_n\,, \tag{54}$$

where $x_0 = y_0$.

The claim is proven by showing that the transition density $f(x_j, t_j|y_0, 0)$ from time 0 to time t_j with $x_j > b(t_j)$ and absorbing barrier $b^\diamond$ is given by

$$f(x_j, t_j|y_0, 0) = \int_{b(t_{j-1})}^{\infty} \dots \int_{b(t_1)}^{\infty} \prod_{i=0}^{j-1} g^+(x_{i+1}, t_{i+1}|x_i, t_i)\, dx_1 \dots dx_{j-1} \tag{55}$$

by induction over j starting from $j = 1$, where $f(x_1, t_1|y_0, 0) = g^+(x_1, t_1|y_0, 0)$ obviously holds. Next, assume that (55) already holds for $j > 1$, and show that it also holds for $j + 1$ arguing by the law of total probability:

$$\begin{aligned} f(x_{j+1}, t_{j+1}|y_0, 0) &= \int_{b(t_j)}^{\infty} g^+(x_{j+1}, t_{j+1}|x_j, t_j)\, f(x_j, t_j|y_0, 0)\, dx_j \\ &= \int_{b(t_j)}^{\infty} g^+(x_{j+1}, t_{j+1}|x_j, t_j) \left(\int_{b(t_{j-1})}^{\infty} \dots \int_{b(t_1)}^{\infty} \prod_{i=0}^{j} g^+(x_{i+1}, t_{i+1}|x_i, t_i)\, dx_1 \dots dx_{j-1} \right) dx_j \\ &= \int_{b(t_j)}^{\infty} \dots \int_{b(t_1)}^{\infty} \prod_{i=0}^{j} g^+(x_{i+1}, t_{i+1}|x_i, t_i)\, dx_1 \dots dx_j\,. \end{aligned} \tag{56}$$

Now use result (55) with $j = n$ to compute the probability to survive until $t_n = T$:

$$\begin{aligned} \mathbb{Q}[y_t > b^\diamond(t),\ 0 \le t \le T] &= \int_{b(t_n)}^{\infty} f(x_n, t_n|y_0, 0)\, dx_n \\ &= \int_{b(t_n)}^{\infty} \int_{b(t_{n-1})}^{\infty} \dots \int_{b(t_1)}^{\infty} \prod_{i=0}^{n-1} g^+(x_{i+1}, t_{i+1}|x_i, t_i)\, dx_1 \dots dx_{n-1}\, dx_n\,. \end{aligned} \tag{57}$$

III Approximate solution for barrier b. The approximate barrier $b^\diamond$ is already identical to b at the points $t_0, \ldots, t_n$. For a given approximation error ε on a subinterval the auxiliary time steps are chosen according to Appendix B.2. For our secification of $\sigma^2(t)$, $r(t)$ and $b(t)$ it can be shown that $|\bar{b}' - (\bar{b}^\diamond)'|_2^2$ goes to 0 if the dissection points are chosen properly and their number n is increased to infinity. The barrier b and thus also the desired survival probability can be approximated to arbitrary precision, cf. Proposition 2.

Note that the same arguments are valid for survival probabilities under $\mathbb{P}$ since the Green function still solves the Kolmogorov equations if $r(t)$ is replaced by $\mu(t)$.

D Figures

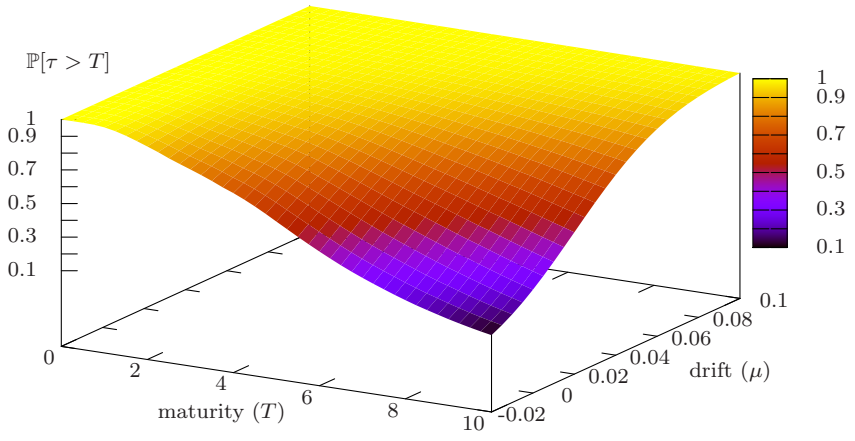

(a) TIT $\mathbb{P}$-Measure Survival Probability

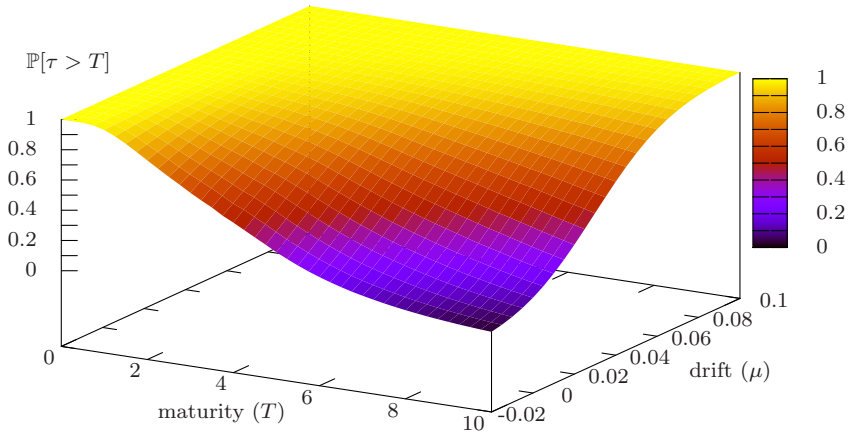

(b) DCX $\mathbb{P}$-Measure Survival Probability

Figure 5: **Survival Probabilities under $\mathbb{P}$ for Varying Asset Drift:** The figure displays survival probabilities under the physical measure $\mathbb{P}$ as a function of the drift μ of the asset value. Both figures are generated using the cross section of CDS maturities observed on the first day in our sample. The "maturity" axis denotes the term (in years).

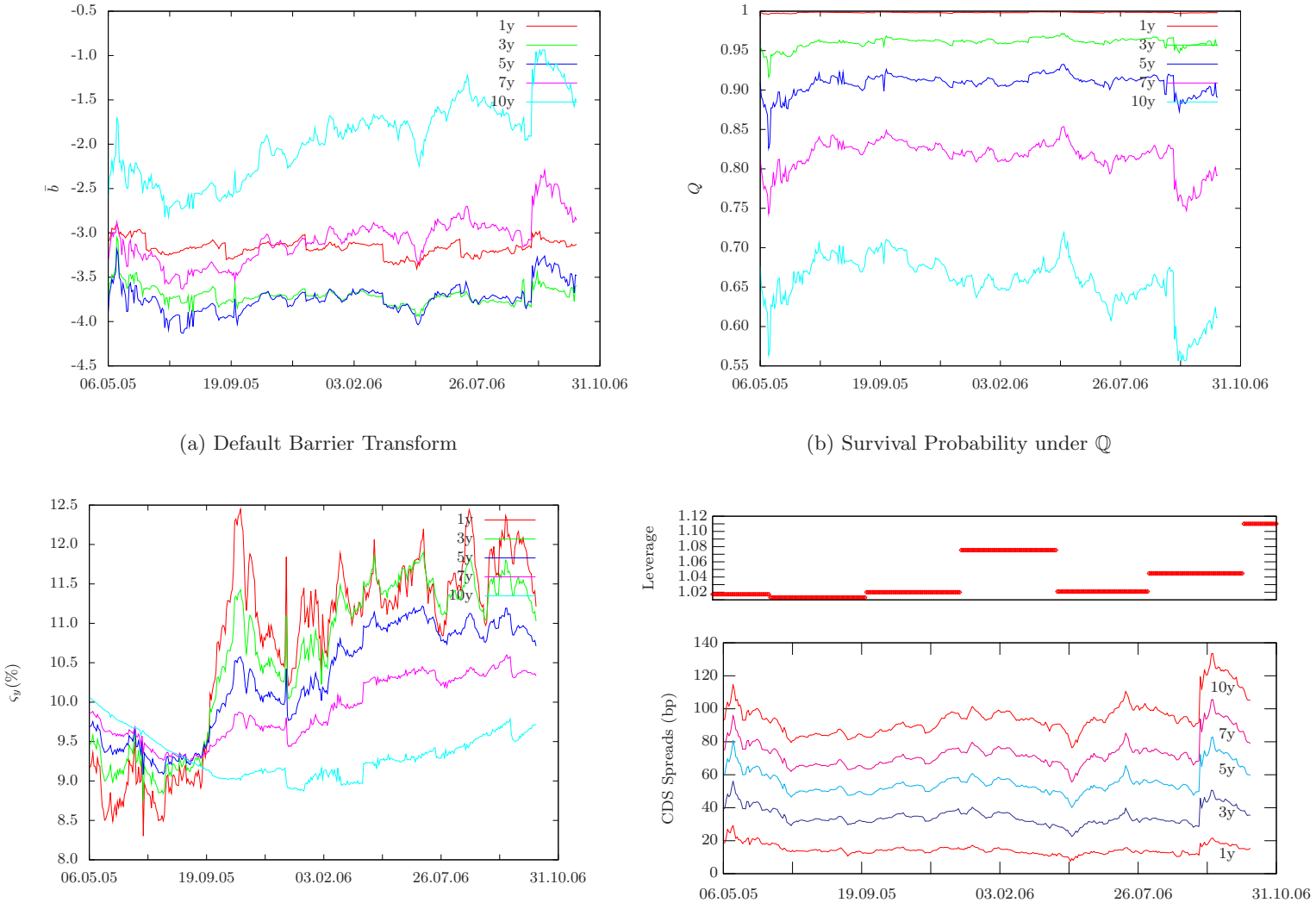

(a) Default Barrier Transform

(b) Survival Probability under $\mathbb{Q}$

(c) Asset Volatility

(d) CDS Spreads and Leverage Ratio

Figure 6: **Input Data and Implied Default Barrier for *Telecom Italia SpA*:** The figure displays (a) the default barrier implied by (c) asset volatilities and (b) default probabilities under $\mathbb{Q}$ resp. (d) daily premia (in bp) of CDS contracts written on *Telecom Italia SpA* between May 6$^{\text{th}}$, 2005 and October 31$^{\text{st}}$, 2006. The date axis denotes the observation period. "Leverage" is the ratio between face value of debt and market value of equity, here the debt-to-market-cap item from Bloomberg.

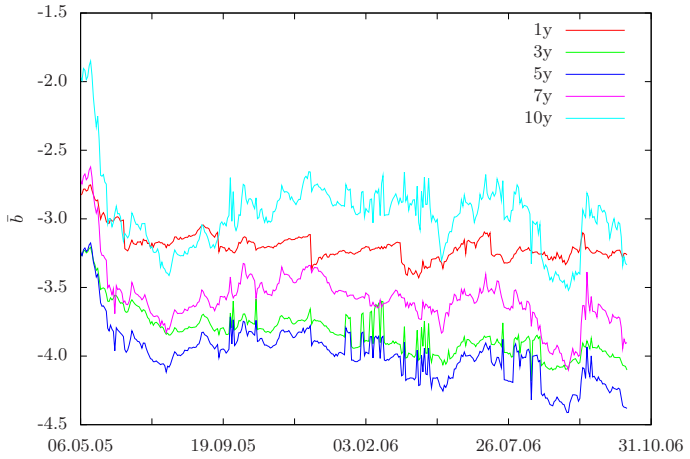

(a) Default Barrier Transform

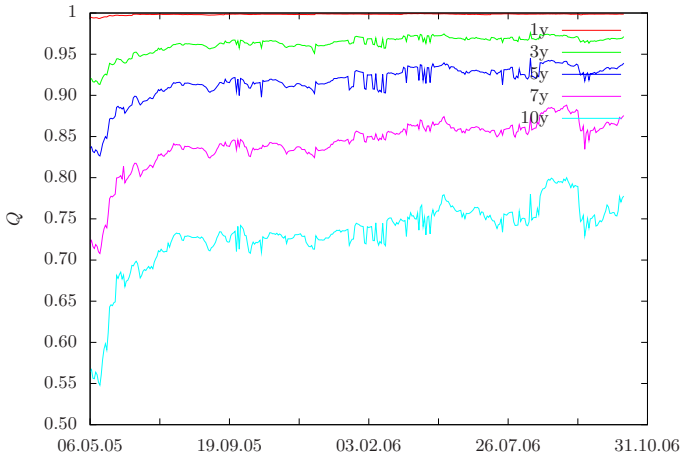

(b) Survival Probability under $\mathbb{Q}$

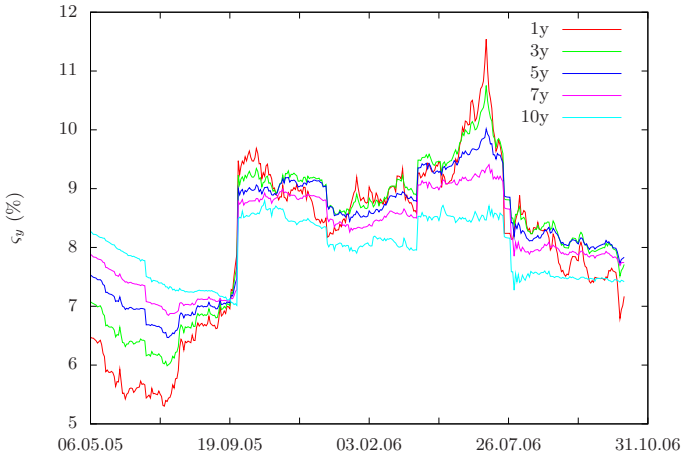

(c) Asset Volatility

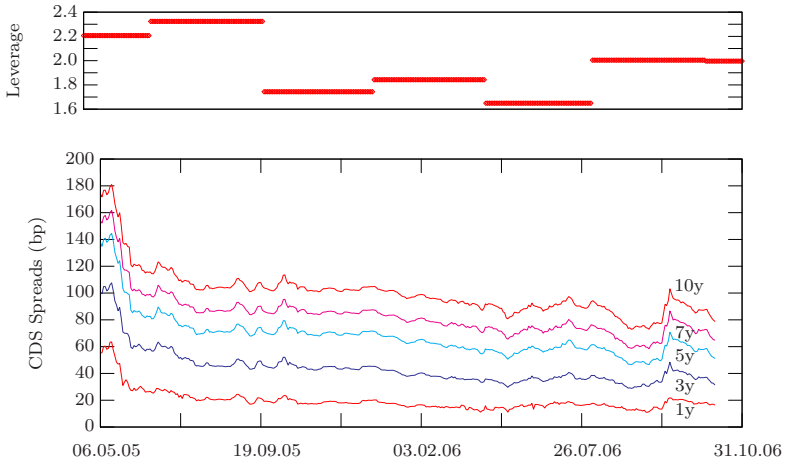

(d) CDS Spreads and Leverage Ratio

Figure 7: **Input Data and Implied Default Barrier for *Daimler Chrysler AG*:** The figure displays (a) the default barrier implied by (c) asset volatilities and (b) default probabilities under $\mathbb{Q}$ resp. (d) daily premia (in bp) of CDS contracts written on *Daimler Chrysler AG* between May 6$^{\text{th}}$, 2005 and October 31$^{\text{st}}$, 2006. The date axis represents the observation period. "Leverage" is the ratio between face value of debt and market value of equity, here the debt-to-market-cap item from Bloomberg.